# Proton decay spectroscopy of <sup>28</sup>S and <sup>30</sup>Cl

S. A. Gillespie, <sup>1,\*</sup> K. W. Brown, <sup>1,2</sup> R. J. Charity, <sup>3</sup> L. G. Sobotka, <sup>3</sup> A. K. Anthony, <sup>1</sup> J. Barney, <sup>1</sup> A. Bonaccorso, <sup>4</sup> B. A. Brown, <sup>1,5</sup> J. Crosby, <sup>1</sup> D. Dell'Aquila, <sup>1</sup> J. Elson, <sup>3</sup> J. Estee, <sup>1</sup> A. Gade, <sup>1,5</sup> M. Ghazali, <sup>1</sup> G. Jhang, <sup>1</sup> Y. Jin, <sup>6</sup> B. Longfellow, <sup>1,5</sup> W. G. Lynch, <sup>1,5</sup> J. Pereira, <sup>1</sup> M. Spieker, <sup>1</sup> S. Sweany, <sup>1</sup> F. C. E. Teh, <sup>1</sup> A. Thomas, <sup>3</sup> M. B. Tsang, <sup>1</sup> C. Y. Tsang, <sup>1</sup> D. Weisshaar, <sup>1</sup> H. Y. Wu, <sup>6</sup> and K. Zhu <sup>1</sup> National Superconducting Cyclotron Laboratory, Michigan State University, East Lansing, MI 48824, USA <sup>2</sup> Department of Chemistry, Michigan State University, East Lansing, Michigan 48824, USA <sup>3</sup> Departments of Chemistry and Physics, Washington University, St. Louis, Missouri 63130, USA <sup>4</sup> Istituto Nazionale di Fisica Nucleare, Sezione di Pisa, Largo B. Pontecorvo 3, 56127 Pisa, Italy <sup>5</sup> Department of Physics and Astronomy, Michigan State University, East Lansing, Michigan 48824, USA <sup>6</sup> School of Physics and State Key Laboratory of Nuclear Physics and Technology, Peking University, Beijing 100871, China (Dated: April 8, 2022)

States in  $^{28}$ S and  $^{30}$ Cl have been studied using one- and two-proton decay spectroscopy. In the first spectrometer setting, states in  $^{28}$ S were populated following one-neutron knockout from a fast  $^{29}$ S beam. Three new states are observed in  $^{28}$ S from one- and two-proton decay. For the two-proton case the nature of the decay was investigated and found to proceed via sequential two-proton emission. For the second setting, states in  $^{30}$ Cl were populated via one-proton knockout from a fast  $^{31}$ Ar beam. The decay energy of the ground and first excited state were measured, with the ground-state decay energy found to be in disagreement with a previous measurement. The spin and parity of these two  $^{30}$ Cl states were inferred from shell-model calculations.

### I. INTRODUCTION

The ground and excited states of isotopes near or beyond the proton dripline decay predominantly via the emission of protons and other charged particles. Using resonance decay spectroscopy, wherein all decay products are detected, allows for the measurement of excitation energies in the parent nuclei. In cases in which the decay involves more than two fragments, such as two-proton decay, the energy and angular correlations between the fragments give information about the nature of the decay, whether it proceeds promptly or sequentially via an intermediate state [1]. Using proton decay spectroscopy we have studied states in <sup>28</sup>S and <sup>30</sup>Cl.

States in <sup>28</sup>S have previously been investigated via Coulomb excitation [2, 3] and knockout reactions [4]. This nucleus has been primarily studied at low excitation energy, focused specifically on the first excited state, in order to investigate a possible sub-shell closure. Data at high excitation energies are limited to a single experiment, which measured 2p-decay following Coulomb excitation of a <sup>28</sup>S beam [3]. Due to the experimental resolution and limited statistics, it was not possible to resolve any states, however 2p-decay was observed in the excitation energy region from 4 - 20 MeV with possible resonance structures at 6.5, 9 and 17 MeV. While individual states could not be observed, the nature of the 2p-decay over the full excitation energy region was investigated from the relative angles of the protons. Comparisons with theoretical models showed evidence for both prompt and sequential 2p-decay.

<sup>30</sup>Cl has previously been studied via proton decay spectroscopy at GSI [5]. States in <sup>30</sup>Cl were identified from the 2p sequential decay of  $^{31}$ Ar, with the energies of the states derived from angular correlations between the detected protons and heavy-ion residue, <sup>29</sup>S. A total of five states were reported in that work, the lowest of which was claimed as the ground state. From the decay energy they calculate the proton separation energy of <sup>30</sup>Cl to be -0.48(2) MeV compared to -0.31 MeV obtained from systematics in the 2016 atomic mass evaluation  $[6]^1$ . As part of this study, cluster model calculations were performed which predicted states not observed. Notably, a low-lying  $J^{\pi} = 3^{+}$  excited state is predicted to exist whose energy is 90 keV above the 2<sup>+</sup> ground state. The existence of these two states is expected as the mirror (<sup>30</sup>Al) has two states separated by 243.9 keV albeit with their order reversed [8]. The authors of [5] also suggest that the ground state might consist of two components. In this work, we present new data on <sup>28</sup>S and <sup>30</sup>Cl, observing several new states in <sup>28</sup>S and showing evidence that the structure previously identified as the <sup>30</sup>Cl ground state is an unresolved doublet.

#### II. EXPERIMENT

Proton decay was studied at the National Superconducting Cyclotron Laboratory (NSCL) at Michigan State University using the invariant-mass method. Secondary beams of  $^{29}\mathrm{S}$  and  $^{31}\mathrm{Ar}$  were produced from fragmentation reactions of a 150-MeV/u primary beam of  $^{36}\mathrm{Ar}$  on a  $^{9}\mathrm{Be}$ 

<sup>\*</sup> stephen.gillespie.90@gmail.com

<sup>&</sup>lt;sup>1</sup> The mass of <sup>30</sup>Cl in the NUBASE 2020 evaluation [7], uses the value from [5].

target. Following fragmentation the secondary beams of interest are filtered by the A1900 fragment separator [9] and transported to a target chamber located at the entrance of the S800 spectrograph [10]. Two spectrograph settings were used. For the first setting, the momentum acceptance of the S800 was set for  $^{28}\mathrm{S}$  residuals and for the second setting for <sup>29</sup>S residuals. Particle Identification (PID) of the secondary beam is performed event-byevent using the time of flight (ToF) between the A1900 focal plane and the object (Obj) position of the S800. The secondary beams undergo reactions on a 0.5 mm thick <sup>9</sup>Be target located within the target chamber with the reaction products decaying via one and two-proton decay (1/2p-decay). Protons are detected and identified with a Si-CsI(Tl) array consisting of a 1-mm-thick Micron S4-type double-sided silicon strip detector (DSSD) [11]. The DSSD with 128 concentric rings and 128 annular sectors, provided the fine-grain position information for the emitted protons. The S4 is backed by 20 CsI(Tl) detectors arranged in two concentric rings with 4 inner and 16 outer detectors. An example PID plot for the Si-CsI(Tl) is shown in Fig. 1. The Si-CsI(Tl) array was located at a distance of 331 mm and 517 mm downstream of the target position for the two S800 settings. An aluminium absorber is placed in front of the DSSD to both prevent scattered beam particles from hitting the detector and to ensure the high-energy protons stop in the CsI(Tl). Following the proton decay the residues are detected by both the S800 and an array of scintillating fibers, arranged into X and Y planes, located directly behind the Si-CsI(Tl) array. The fiber array consists of 0.25-mm-thick BC-400 type square scintillating fibers and is used to determine the angles of the scattered residues. The signals from each fiber layer are amplified using a segmented photomultiplier tube and read out at the corners via a resistive anode. The S800 itself is used to identify the reaction products from the ToF through the spectrometer and the energy loss in an Ionisation Chamber (IC). In addition to the charged-particle detectors, the CAESAR [12] CsI(Na) photon detection array was positioned around the target to identify proton decays populating excited states which  $\gamma$  decay.

### III. DATA AND ANALYSIS

### A. Invariant-Mass Method

Excited-state energies were determined in this work using the invariant-mass method (IMM). By measuring the energy of all particles and the relative angles between the protons, in the Si-CsI(Tl), and the recoiling residues, in the fiber array, the total decay energy can be reconstructed from which the energy of excited states can be determined. In the case where the parent decays to a particle-bound excited state in the daughter, the invariant masses will be incorrect. CAESAR however was used to detect  $\gamma$  rays from the decay of excited states, and as-

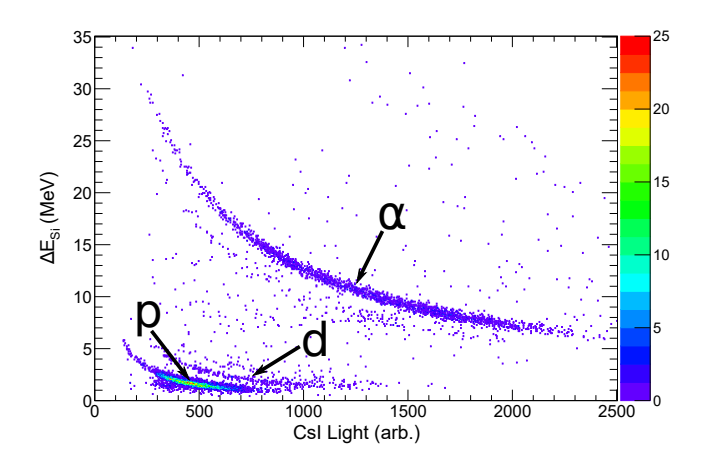


FIG. 1. Example Si-CsI(Tl) PID plot showing the energy deposited in the S4 silicon detector ( $\Delta E_{Si}$ ) vs energy deposited in a CsI(Tl) crystal. The silicon energy has been calibrated and the CsI(Tl) energy is uncalibrated. Different bands are labeled by their corresponding isotope

sociate them with specific invariant-mass peaks to correct the excited-state energy.

## B. Experimental Method

To identify states in this work the total decay energy,  $E_T$  is first reconstructed using the IMM. Energies are obtained from fits of the decay energy spectrum which comprises one or more Gaussian functions on a background. The source of this background is due to non-resonant decay and from broad states. To determine if the peaks in this work are single narrow resonances, broad states or from multiple peaks the following procedure was employed: First, the experimental resolution is determined from simulations, benchmarked on previous IMM measurements of <sup>16</sup>Ne and <sup>18</sup>Mg [13], which were performed using the same Si-CsI(Tl) array. The experimental resolutions obtained were approximately 0.18 and 0.11 MeV for the two Si-CsI(Tl) target distances 331 mm and 517 mm. R-Matrix calculations are performed to determine the state widths and are compared to the experimental resolution. Provided the estimated upper limit of the width of the state is small compared to the experimental resolution, the decay energy spectrum is fit with the Gaussian widths fixed from simulations. In addition, we also search for coincident  $\gamma$  rays in CAESAR which would suggest the 1/2p-decays proceed to an excited state in the daughter. The total excitation energy is then obtained from the sum of the decay energy, the one or two-proton separation energies,  $S_p$  and  $S_{2p}$ , and the energy of any coincident  $\gamma$  ray.

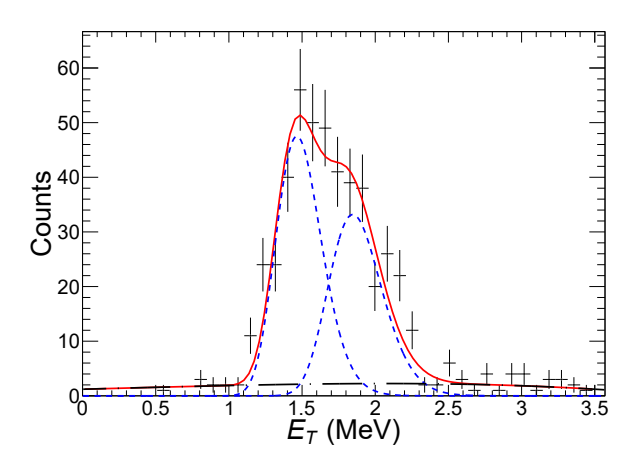


FIG. 2. Total decay kinetic energy  $E_T$  obtained with the invariant-mass method for the  $^{28}{\rm S} \rightarrow ^{27}{\rm P} + 1p$  decay channel. The experimental data are shown by the data points. The spectrum has been fit (in red) with a function consisting of two Gaussian functions (blue dashed curves) plus background (black dot-dashed).

#### C. $^{28}$ S

States in  $^{28}$ S were populated via 1n knockout of the  $^{29}$ S secondary beam and studied via both 1- and 2p-decay. For the 1p-decay case, the recoiling  $^{27}$ P isotopes were at the edge of the momentum acceptance of the S800 resulting in its low detection efficiency. The reconstructed decay-energy spectrum for the 1p-decay of  $^{28}$ S is shown in Fig. 2. The spectrum is fit with two Gaussian peaks, from which decay energies of  $E_T = 1.476(25)$ , 1.860(36) MeV are obtained. No evidence of coincident  $\gamma$  rays were seen in CAESAR suggesting they decay directly to the ground state in  $^{27}$ P. Using the proton separation energy from the most recent mass evaluation [7],  $S_p(^{28}S) = 2.56(16)$  MeV, we calculate these states to have excitation energies  $E_x = 4.04(16)$  and 4.42(16) MeV.

To determine spins for these states we compare them to both states in the mirror nucleus ( $^{28}$ Mg) as shown in Fig. 3 and to shell model calculations performed using the USDC Hamiltonian [14]. Spectroscopic factors were calculated for the 1n knockout to both states and for each state only one spin assignment had a significant spectroscopic factor. Based on these we suggest that the spins of the 4.04(16) and 4.42(164) MeV states are  $J^{\pi}=4^+$  ( $C^2S=0.042$ ) and  $2^+$  ( $C^2S=0.255$ ) respectively. For the 4.04(16) MeV state we note that it is predicted to decay predominantly to the  $3/2^+$  state in  $^{27}$ P which we do not observe. The energy of this decay,  $E_T=0.346$  MeV, however would be outside our experimental acceptance.

The reconstructed decay-energy of the 2p-decay of  $^{28}$ S is shown in Fig. 4 and is fit to obtain a peak energy of  $E_T = 1.905(17)$  MeV. In the  $\gamma$ -ray spectrum there is evidence of the 1797 keV  $2^+ \to 0^+$  transition. This is however, in coincidence to the high-energy background, from which

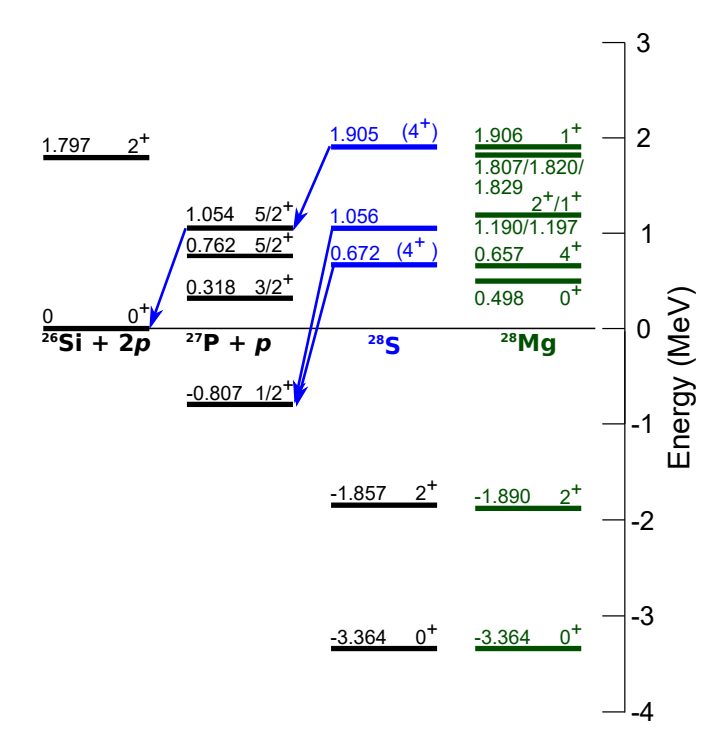


FIG. 3. Partial level scheme for the for 1- and 2p-decay of <sup>28</sup>S. Newly identified levels are shown in blue. For comparison states in the mirror nucleus <sup>28</sup>Mg are shown. The energy of the states in <sup>28</sup>Mg are adjusted by  $S_{2p}(^{28}S) = 3.36(16)$  MeV. Data were taken from Nuclear Data sheets [8].

individual states cannot be resolved. For the main peak, there is no evidence of a  $\gamma$  ray transition in CAESAR, therefore the excitation energy of this state, including  $S_{2p}(^{28}S) = 3.36(16) \text{ MeV } [7], \text{ is calculated to be } 5.27(16)$ MeV. The decay of this state was investigated from the three-particle-decay correlations to determine if the decay is prompt or sequential through an intermediate <sup>27</sup>P state. The energy of the possible intermediate state was reconstructed from the invariant-mass of the <sup>26</sup>Si recoil and either of the protons. The exact energy of the intermediate state could not be determined, but it suggests the intermediate state of the sequential decay would be at approximately half the total decay energy. A possible candidate for this intermediate state was observed via a recent  $\beta$ -decay study of <sup>27</sup>S [15]. A  $5/2_2^+$  state was observed at 1.861(13) MeV in <sup>27</sup>P, corresponding to decay energies of 0.86 and 1.06 MeV for the first and second decay steps respectively. Simulations for the decay correlations, namely the Jacobi "T" and "Y" distributions are shown in Fig. 5 along with the experimental data. For the case of sequential decay, the intermediate state is assumed to be the 1.861(13) MeV state found in  $^{27}$ P following the  $\beta$  decay of <sup>27</sup>S [15]. The shape of the experimental distribution suggests the decay of the 5.27 MeV state is an example of sequential 2p-decay.

To determine the spin of this state, experimental longitudinal-momentum distributions are compared to calculations for knockout of a  $1d_{5/2}$  or  $2s_{1/2}$  neutron. Be-

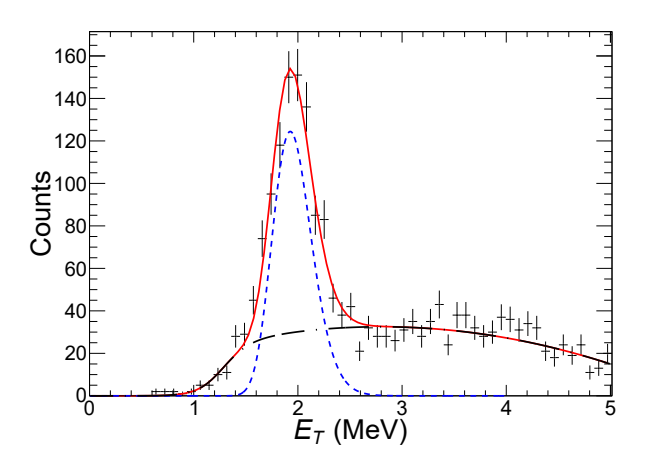


FIG. 4. Total decay kinetic energy  $E_T$  obtained with the invariant-mass method for the  $^{28}\mathrm{S} \to ^{26}\mathrm{Si} + 2p$  decay channel. The experimental data are shown by the data points. The spectrum has been fit (in red) with a function consisting of a Gaussian function (blue dashed curves) plus background (black dot-dashed).

cause of the relatively low incident energy and the evident asymmetry of the experimental spectra, model core parallel momentum distributions were calculated according to the Semiclassical Transfer-to-the-Continuum (STC) method [16, 17]. The STC method takes into account energy and momentum conservation between the initial nucleon bound state and final continuum state with respect to the target. The nucleon-<sup>9</sup>Be final-state interaction was treated by using the energy dependent optical model potential of Ref. [18]. The initial states were calculated as single-particle states in Woods-Saxon potentials with fixed geometry ( $r_0 = 1.25 \text{ fm}, a = 0.7 \text{ fm}$ ) and depth fitted to reproduce the experimental nucleon separation energy. Under the core-spectator hypothesis the STC method is equivalent to a fully quantum-mechanical model [19] and at high energy transitions to the eikonal treatment [20, 21]. The calculations were used as an input to a Monte-Carlo simulation to account for the effects of target interaction point and the experimental resolution. Fig. 6 shows the overlay of the experimental distribution with this simulation. The simulations indicate the state is populated following the knockout of a  $1d_{5/2}$ neutron, which constrains the spin of this state to  $J^{\pi}$  =  $(0-5)^+$ . Shell model calculations were also performed to further constrain the spin of this state [14]. Only one spin assignment was found to have a significant spectroscopic factor and based on this we suggest the state would be most likely a  $4^+$  state ( $C^2S = 0.255$ ) and would predominantly decay to the  $5/2^+_2$  state in  $^{27}$ P. This is consistent with what is seen experimentally suggesting the spin of the 5.27-MeV state is  $J^{\pi} = 4^{+}$ .

TABLE I. List of levels observed in  $^{28}$ S and  $^{30}$ Cl in this work. Decay energies are measured in this work, with the excitation energies of the states in  $^{28}$ S calculated using the values  $S_p(^{28}S) = 2.56(16)$  MeV and  $S_{2p}(^{28}S) = 3.37(16)$  MeV obtained in the latest mass evaluation [7]. Spin parity assignments are made based on comparisons with mirror nuclei [8], longitudinal-momentum distributions [16, 17] and shell model calculations [14], with the details described in the text.

Nucleus	$E_T \text{ (MeV)}$	$E_x \text{ (MeV)}$	$J^{\pi}$	Decay Mode
$^{28}\mathrm{S}$	1.476(25)	4.036(162)	$4^{+}$	1p-decay
$^{28}S$	1.860(36)	4.42(164)	$2^{+}$	1p-decay
$^{28}S$	1.905(17)	5.275(161)	$4^+$	2p-decay
$^{30}Cl$	0.364(29)	0.0	$3^+$	1p-decay
<sup>30</sup> Cl	0.617(35)	0.253(45)	2+	1p-decay

## D. 30Cl

The ground and first excited state in <sup>30</sup>Cl were populated via 1p knockout of a  $^{31}$ Ar secondary beam. Due to the low expected energy difference between the ground and  $1^{st}$  excited state, the distance between the reaction target and the Si-CsI(Tl) array was increased to 517 mm. This improves the angular resolution of the array and subsequently offers improved energy resolution, albeit at the expense of efficiency at higher decay energies. The reconstructed decay-energy,  $E_T$ , spectrum is shown in Fig. 7. From the fit of the spectrum we measure the decay energies of these two states to be  $E_T(g.s.) = 0.364(29) \text{ MeV}$ and  $E_T(1^{st}) = 0.617(35)$  MeV. No  $\gamma$  rays were observed in coincidence, indicating that  $S_p(^{30}\text{Cl}) = -0.364(29)$  MeV and  $E^*(1^{st}) = 0.253(45)$  MeV. The decay energies observed here are found to be in disagreement with the GSI work [5], who measured the decay energy of the ground state to be 0.48(2) MeV. We note, however that the average of the decay energies in this work is 0.49(12) MeV which would suggest the previously reported ground state was an unresolved doublet. The  $S_p$  value obtained in this work is consistent within  $2\sigma$  of the value obtained from systematics in the 2016 mass evaluation, -0.31 MeV [6].

To determine the spins of the two states, we calculate the relative population of the two states in this work and compare this to predictions from shell-model calculations using the USDC Hamiltonian [14]. Accounting for detector efficiencies we determine the intensity ratio of the two states to be 0.585(22):0.415(16). For the shell model the predicted ratio of two states, with  $J^{\pi}=3^+$  and  $2^+$  is found to be 0.634:0.366. Comparing these ratios we tentatively assign the spins of these states to be  $J^{\pi}(g.s.)=3^+$  and  $J^{\pi}(1^{st})=2^+$ . This ordering is in disagreement with the calculations of [5], but is consistent with that of its mirror nucleus  $^{30}$ Al [8].

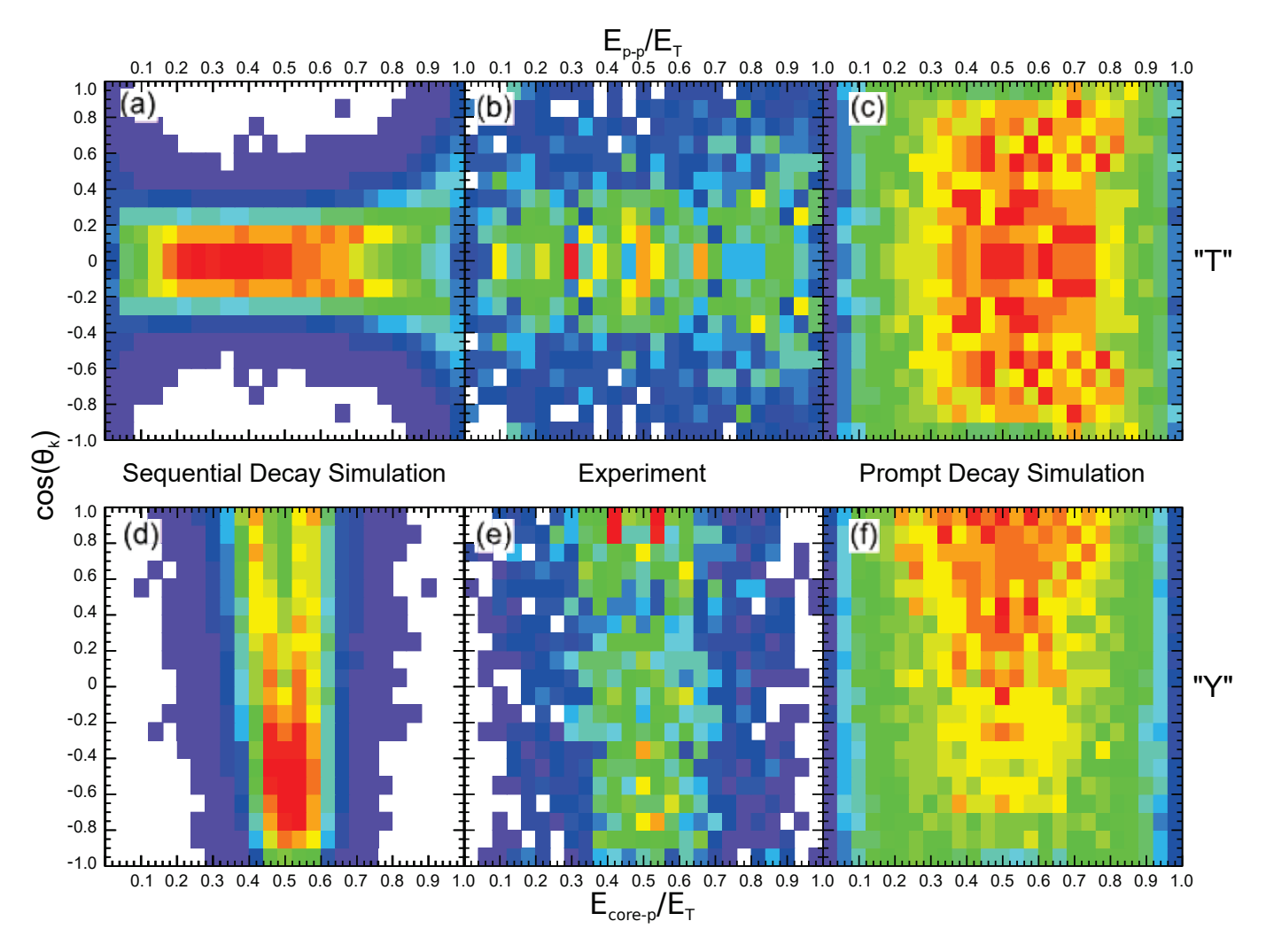


FIG. 5. Comparison of the experimental Jacobi (b) "T" and (e) "Y" correlation distributions for the 5.27 MeV state in <sup>28</sup>S to those from a sequential decay simulation [(a) and (d)] and a three-body model [(c) and (f)]. The effects of the detector efficiency and resolution in the theoretical distributions have been included via Monte Carlo simulations. For the sequential decay case, the decay proceeds through a 1.861(13) MeV state in <sup>27</sup>P [15]. Data is not shown to scale.

### IV. CONCLUSION

States in  $^{28}$ S and  $^{30}$ Cl have been identified via one- and two-proton decay spectroscopy. For the case of  $^{28}$ S two states were identified via 1p-decay, with another state identified via 2p-decay. Comparisons with Monte-Carlo simulations suggest that the 2p-decay is sequential via a intermediate state in  $^{27}$ P. Based on comparisons with longitudinal-momentum calculations and shell model calculations we suggest the spin of this state to be  $J^{\pi}=4^+$ . In  $^{30}$ Cl we have measured the decay energy of the ground and first excited states. The ground state is found to be in disagreement with a previous measurement and the first excited state has been measured for the first time. The disagreement with the previous measurement

is likely due to them observing the ground and first excited state as a single state. From comparisons with shell model calculations the spins of the ground and first excited state were determined to be  $J^{\pi}=3^{+}$  and  $2^{+}$  respectively.

### ACKNOWLEDGMENTS

This work was supported by the U.S. Department of Energy, Office of Nuclear Physics under Grant No. DE-FG02-87ER-40316 and DE-SC0020451 (NSCL) and the U.S. National Science Foundation under Grant No. PHY-1565546

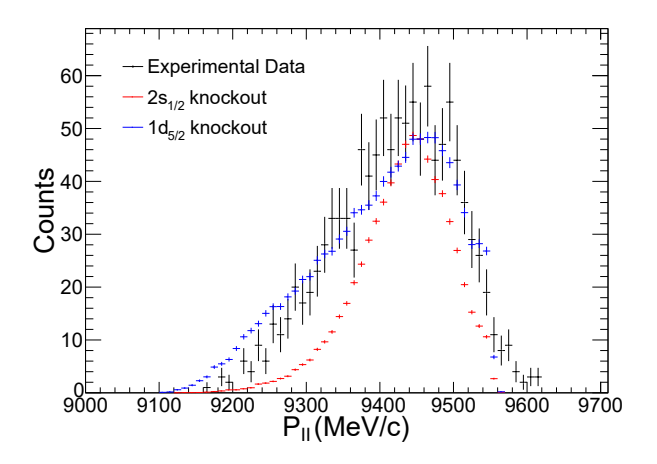


FIG. 6. Longitudinal-momentum distributions of reconstructed residuals following 1n knockout from a  $^{29}\mathrm{S}$  projectile. The experimental distribution (in black) is gated on the peak shown in Fig. 4. Monte-Carlo simulations have been performed for the case of  $1\mathrm{d}_{5/2}$  or  $2\mathrm{s}_{1/2}$  neutron knockout and are shown as blue and red data points respectively. The simulations have been scaled to the experimental peak height.

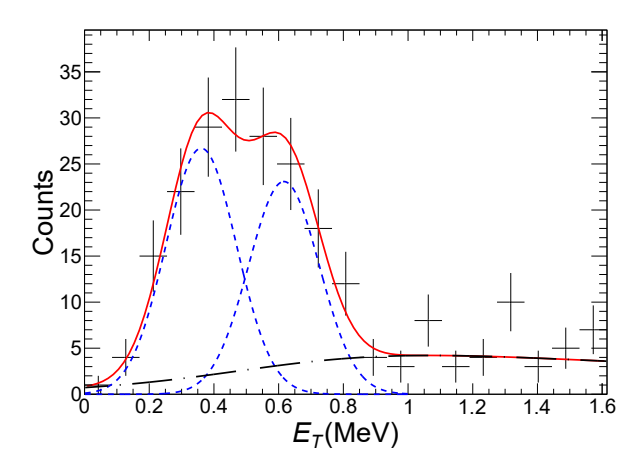


FIG. 7. Total decay kinetic energy  $E_T$  obtained with the invariant-mass method for the  $^{30}{\rm Cl} \rightarrow ^{29}{\rm S} + 1p$  decay channel. The experimental data are shown by the data points. The spectrum has been fit (in red) with a function consisting of two Gaussian functions (blue dashed curves) plus a background (black dot-dashed).

- [3] X. X. et al., Phys. Lett. B **727**, 126 (2013).
- [4] K. Y. et al., Phys. Rev. C 74, 021303 (2006).
- [5] t. I. Mukha, Phys. Rev. C 98, 064308 (2018).
- [6] M. Wang, G. Audi, F. Kondev, W. Huang, S. Naimi, and X. Xu, Chinese Phys. C 41 (2017).
- [7] F. Kondev, M. Wang, W. Huang, S. Naimi, and G. Audi, Chinese Phys. C 45 (2021).
- [8] M. S. Basunia, Nuclear Data Sheets 114, 1189 (2013).
- [9] D. Morrissey, B. Sherrill, M. Steiner, A. Stolz, and I. Wiedenhoever, Nucl. Instrum. Methods Phys. Res. Sec. B 204, 90 (2003).
- [10] D. Bazin, J. Caggiano, B. Sherrill, J. Yurkon, and A. Zeller, Nucl. Instrum. Methods Phys. Res. Sec. B 204, 629 (2003).
- [11] M. S. Ltd., "Micron Catalogue," (2018).
- [12] D. Weisshaar, A. Gade, T. Glasmacher, G. Grinyer, D. Bazin, P. Adrich, T. Baugher, J. Cook, C. Diget, S. McDaniel, A. Ratkiewicz, K. Siwek, and K. Walsh, Nucl. Instrum. Methods Phys. Res. Sec. A 624, 615 (2010).
- [13] Y. J. et al., Phys. Rev. Lett. 127, 262502 (2021).
- [14] A. Magilligan and B. A. Brown, Phys. Rev. C 101, 064312 (2020).
- [15] L. J. S. et al. (RIBLL Collaboration), Phys. Rev. C 99, 064312 (2019).
- [16] A. Bonaccorso and D. M. Brink, Phys. Rev. C 38, 1776 (1988).
- [17] A. Bonaccorso and D. M. Brink, Phys. Rev. C 44, 1559 (1991).
- [18] A. Bonaccorso and R. J. Charity, Phys. Rev. C 89, 024619 (2014).
- [19] J. Lei and A. Bonaccorso, Phys. Lett. B 813, 136032 (2021).
- [20] A. Bonaccorso, Prog. Part. and Nucl. Phys. 101, 1 (2018).
- [21] A. Bonaccorso and D. M. Brink, Eur. Phys. J 57, 171 (2021).